Sensors & Transducers, Vol. 208, Issue 1, January 2017, pp. 1-6

www.sensorsportal.com

Sensors & Transducers

Published by IFSA Publishing, S. L., 2017
http://www.sensorsportal.com

Gas Sensors Built with Nanomaterials and Provided with a Heating Double Purpose Hot-plate

[1, 2] Cristian L. ARRIETA, [3] Mario F. BIANCHETTI, [1] Claudio A. GILLARI, [1] Lidia T. ALANIZ, [2] Héctor A. LACOMI, [2] Matías A. MARANDO and [3] Noemí E. WALSÖE DE RECA

[1] Microelectronics Division, DEA-CITEDEF, Villa Martelli, Bs.As., Argentina
[2] Electronics Dept. (SyCE), National Technology University UTN FRH, Paris 532, (1706) Mariano J. Haedo, Prov. Bs.As., Argentina
[3] DEINSO-Materials Department-CITEDEF (UNIDEF-MINDEF-CONICET), Juan Bautista de La Salle 4387 (B1603ALO). Villa Martelli, Prov. Bs. As., Argentina
[3] Tel.: 54 11 4709-8100, fax: 54 11 4709-8158
E-mail: walsoe@citedef.gob.ar, carrieta@citedef.gob.ar

Received: 4 October 2016 /Accepted: 30 December 2016 /Published: 31 January 2017

Abstract: Pure or doped SnO_2, has been used to build resistive type gas sensors from several decades. This subject has been retaken using pure or doped nanocrystalline SnO_2 to build the sensors, finding considerable advantages in devices performance. The sensors working temperature (Tw) decreases from (350-450) ºC to (180-200) ºC in comparison with that of devices built with microcrystalline conventional material. Sensitivity of sensors built with nanocrystalline material in comparison with that of devices built with conventional microcrystalline material, increases from 30% to 37%. In this work, SnO_2 is synthesized using two different modified techniques based on gel-combustion and reactive oxidation and results of both syntheses are compared. Nanomaterials are characterised with X-ray diffraction (XRD), High Resolution Transmission Electron Microscopy (HRTEM) and Field Emission Electron Scanning Microscopy (FESEM) and absorption techniques (BET). An electronic system, already patented by the authors, enables to alternatively measure the sensor resistivity (which is proportional to the adsorbed gas concentration) and set a constant working temperature, thus contributing to considerably save energy.

Keywords: Resistive gas sensors, MEMS, Nanocrystalline SnO_2, Reactive oxidation synthesis, VOCs.

1. Introduction

Pure or doped SnO_2 semiconductor has been used for many years to build resistive type gas sensors [1-7]. When the size of the oxide particles decreases to the nanometric scale, important changes are observed in gas sensors built with nanocrystalline material directly depending on the oxide crystallite size. An increase of sensitivity (30%-37%) is observed in sensors built with nanocrystalline material in comparison with the sensitivity of sensors built with the same material but microcrystalline. The working temperature (Tw) decreases from (350-450) ºC to a range (180-200) ºC [8-10]. In sensors previously built by the authors, the microcrystalline semiconductor has been deposited on one face of an AlSiMg substrate, building on the opposite face, a heating circuit to reach the high Tw. In this work, the nanosemiconductor is deposited as a MEMS type microheater, which functioning is based on an electronic circuit that

implements a switching logic. This circuit enables to measure the variation of film surface resistivity which is related to the analyte concentration and, conveniently heated, it enables to save energy.

The gas detection process is affected by several factors, among them: the microstructure of the gas adsorbing surface. The metallic oxide previously reacts with the air oxygen forming adsorbates on oxide surface (O^-, O^{2-}, O_2^-) [11-13] of which the most active is O^-. The adsorbates play an important role in the sensing process, covering the semiconductor oxide surface and grain boundaries and reacting at a working temperature: Tw ~ (350-450) ºC if the sensor is built with the microcrystalline semiconducting oxide (SCO). In case of n-type metallic oxides, the adsorbates formation generates a charge space region, resulting in an electron depleted surface layer, due to the electrons transference towards the adsorbates according to:

$$O_2(g) + 2e^- = 2O^- \text{ (adsorb.)} \qquad (1)$$

The charge space depth is a function of the surface covering with the oxygen adsorbates and of the intrinsic electron concentration in the bulk. The n-type SCO resistance is consequently high because a potential barrier is formed by the electronic conduction in each grain boundary [11]. If the sensor is exposed to a reducing gas (i.e. CO) at Tw, the gas reacts with the oxygen adsorbate according to:

$$CO + O^- = CO_2 + e^- \qquad (2)$$

The oxygen adsorbates are consumed in subsequent reactions so as to reach a lower steady state, the potential barrier height decreases and the resistance falls being the resistance variation, the sensor measurement parameter. A simple schematic model of the grain boundary effects on the surface resistivity was proposed by Yamazoe et al. [11] in which it was accepted that the sensor sensitivity increases as the grain size decreases. The sensor sensitivity (S) is defined as:

$S = R_{air} / R_{air+gas}$, where: R_{air} is the resistance in air and $R_{air+gas}$ is the resistance in a gas mixture containing a reducing gas component. The oxygen adsorbates resistivity is a function of the reducing gas type and of sensor temperature.

The microstructure and morphology of Al-doped or In-doped nanocrystalline SnO_2 (with different crystallites size) has been studied, contributing the doping to increase the sensor selectivity to different gases [14]. Nanomaterials were prepared by sol-gel [15] and by reactive oxidation with H_2O_2 [16] and the found similar results were analysed [7, 14]. Characterisation has been performed with X-ray diffraction (XRD), absorption techniques by Brunauer-Emmer-Teller (BET) isotherms and High Resolution Transmission Electron Microscopy (HRTEM). Authors' previous works generated interesting results since the sensors sensitivity increased from 30% to 37% and the Tw considerably decreased from 350 ºC - 450 ºC to 250 ºC - 350 ºC for Al-doped nanocrystalline SnO_2 and, similarly, to 180 ºC - 220 ºC for In-doped nano-SnO_2, corresponding the minor Tw to pure nano-SnO_2 [8-10]. The detection process is also affected by other factors, like the oxide microstructure, among them.

2. Experimental Procedure and Results

2.1. Pure SnO_2 Synthesis

Pure SnO_2 nanopowders were synthesized by two techniques (gel-combustion and reactive oxidation) and results were compared [7]: modified gel-combustion with nitrate-citrate [15] and reactive oxidation with H_2O_2 [16].

The gel-combustion is a fuel rich synthesis [15] beginning with a precursor preparation (an aqueous solution with metallic p/a Sn), 70% - HNO_3 - CH_3COOH and 25% - $NH_4.OH$. Citric acid is the organic fuel with a rate: [Sn/fuel] = 1:6; pH is controlled with $(NH_4)OH$ (approaching to neutrality and maintaining the solution homogeneity). The solution is thermally evaporated till reaching a gel. Upon keeping the heating, the gel is transformed into a dark foam which ignites. The intensive combustion in the final stage is due to a highly isothermic redox reaction which is produced between the oxidant nitrate ions and the organic fuel at ~ 80 °C and ignition is produced at ~200 °C - 300 °C. Combustion usually generates an ignition which is independent of the provided atmospheric oxygen since the foam bubbles are filled either with NH_4NO_3 vapor or with NO_x ($1< x <2$) restricting the oxygen access to the site bottom where the reaction is produced. The combustion duration is short, usually half a minute. The gas liberation produces a fast disintegration of the precursor gel at high temperature causing decomposition. If the oxide contains carbonaceous residues by fuel excess, they must be removed by calcination and nanometric crystallites are produced (9 nm - 15 nm). Parameters to be controlled are: type of organic fuel, combustion temperature and process duration. After the synthesis, the crystallites size and homogeneity, the morphology and the impurities retention during the synthesis process have been carefully evaluated.

In the second method, the $SnCl_2$ reacts with H_2O_2 and the product is afterwards treated with $(NH_4)OH$ in H_2O_2 medium. The stannic acid is produced treating the SnO_2 powder by calcination:

$$SnCl_2 + H_2O_2 \rightarrow SnOCl_2 + H_2O \qquad (3)$$

$$SnOCl_2 + 2(NH_4)OH \xrightarrow{H_2O_2} SnO_3H_2 + 2(NH_4)Cl \xrightarrow{\text{calcin.}} SnO_2 \qquad (4)$$

The oxidative reaction with H_2O_2 disintegrates the product particles generating small crystallites with sizes in a range: 2 nm - 9 nm.

2.2. Synthesis of Doped SnO_2

The gas sensor to detect hydrogen was built with pure nanocrystalline SnO_2 [9]. The device to sense CO (g) ppm was built with Al-doped nanocrystalline SnO_2 [8] and that to sense VOCs was built with In-doped nanocrystalline SnO_2 [10]. The method to prepare the two first materials: pure and Al-doped SnO_2 was gel-combustion using CH_3COOH as fuel, being the crystallite size: 2 nm - 4 nm. In the case of In-doped nanocrystalline SnO_2 [10], the synthesis method consisted in precipitating together $SnCl_2.2H_2O$ and $InCl_3$, in NH_4NO_3 medium to produce the stannic oxi-hydroxide which is intensively oxidized with 30-250 vol. H_2O_2, thus producing stannic acid in nanocrystalline powder. This solution is precipitated with $(NH_4)OH$ to get a homogeneous compound of stannic acid and indium hydroxide, being the resulting crystallite size ~2 nm - 4 nm.

2.3. Nanomaterials Characterisation

The X-ray diffraction enabled to identify the material, to evaluate the crystalline structure and to measure the crystallites size (applying the Scherrer equation); the adsorption BET (Brunauer-Emmer-Teller isotherms) measurements have been used to determine the specific area and the HRTEM, Fig. 1 is a HRTEM micrograph of pure nano-SnO_2 lattice, oriented [101] and the e-diffraction pattern.

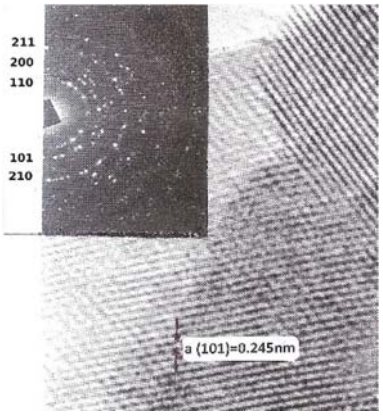

Fig. 1. HRTEM micrograph of pure nano-SnO_2 lattice (calcinated at: 700 °C) oriented along [101] with the electron diffraction pattern. The atomic ordering is clearly resolved.

2.4. Heating Hot-plate and Related Electronics

As it was pointed out before, if the working temperature (Tw) is in the range: 300 ºC-400 ºC, the heater needs a high electric power, which is a problem in the application field. Reliable control of the operating temperature prolongs the life of the assembly sensor-capsule.

The micro hot-plate, used to perform measurement and heating [17], involves a minimal power consumption and exhibits an architecture enabling the manufacture on a MEMS type support. Fig. 2 shows the micro hotplate architecture, which support is a silicon <100> wafer coated with a non-stoichiometric Si_xN_y film. The coating exhibits a low residual stress (< 200 MPa) and 1 micron thick grown by LPCVD enabling the system thermal isolation and the structure resistance and mechanical stability. Square windows: 1.5 mm x 1.5 mm, are usually got.

The micro hotplate, connected to a TO-8 capsule, is shown in Fig. 3. Hot-plates were built with platinum including a TiO_2 adherent interface. The hot-plate consists of a micromachined silicon support and windows are got by wet etching technique with KOH. The Si_xN_y substrate coating stops the etching of micromachining process and acts as thermal isolation between the hot zone and the substrate body which is joined to the capsule. To reach an optimal thermal isolation it is of the highest importance to get reliable welding between the capsule contacts and the sensor (on the wafer). A platinum heater with double-meander structure (heating – pick-up contacts) is integrated to the Si_xN_y film.

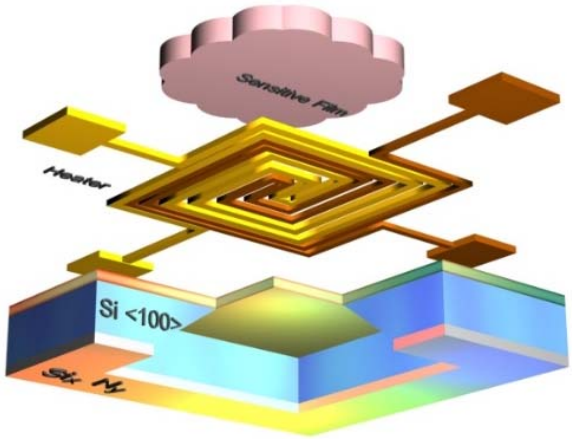

Fig. 2. Architecture of the MEMS hot-plate.

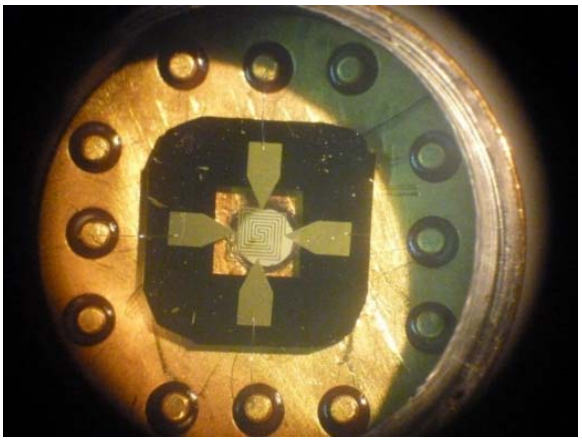

Fig. 3. Microheater.

The double meander structure is centered in the window of the Si_xN_y membrane released from the substrate, by micromachining the <100> Si. This arrangement is used to improve the device thermal efficiency with regards to minimal power consumption [18-20].

The double meander structure is used to heat the sensitive film and to extract the signal. This new structure not only achieves a performance similar to conventional sensors heaters deposited on alumina substrates, but also reduces 10-15 times the device power consumption [20]. Otherwise, the thermal and electrical contact is directly produced with the nanostructured sensitive film, being the film printed with a thick film technology through handicraft techniques, similar to those of screen printing [20]. To explain the use of the Pt double meander as heater and as contact to pick-up the signal, the ad-hoc electronics as described in [17, 19] is considered, Fig. 4.

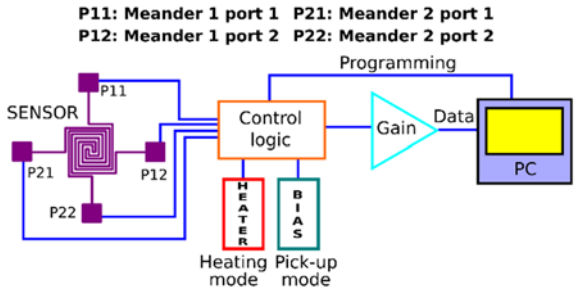

Fig. 4. Electronic control system diagram.

The portable electronic system consists of a microcontroller and discrete electronics components [17]. The description of the elements of the diagram shown in Fig. 4 is detailed:

- PC (data acquisition and calculation): it enables the storage of resistivity values of the sensitive film in function of time to transform these values into the concentration of the gas to be measured. The signal is filtered to reduce measurement noise. The processed data are then transmitted to an external device for later use.
- Gain: amplifies and conditions the signal picked up by the sensitive film, which is then acquired and processed by the PC block.
- Control logic: switches the heater-contact between both two functions (sensitive film heater or contacts).
- Heating: includes the electronic components that apply the necessary power level (temperature) which is convenient to reach the optimal response of the sensitive semiconductor film (Tw).
- Bias: electronic circuit that generates the SnO_2 film bias.
- Sensor (heating-contacts): sensitive film printed on the double meander (double purpose).

The logic obeying the device functioning is as follows: the control logic switches the connection of the double meander electrodes to use them as heaters or contacts capable of picking up the signal according to a predetermined timing stored in the system memory. The working principle is based on the application of a simple pulsed type strategy [19]: for a time lapse (ms), the sensor electrodes are excited through the heating block (which supplies the necessary power for the correct operation of the SnO_2 sensing film). In this heating stage, the two resistors which form the double meander are connected in series. The Si_xN_y membrane exhibits a thermal isolation enabling, once removed the heating power, to maintain the sensor temperature during a short lapse (ms). After heating, the control logic switches the double meander contacts to the pick-up mode enabling the bias block to excite the terminals with convenient bias levels on the sensitive film. The double meander structure and the connection of the electrodes in heating and pick-up modes are shown in Figs. 5a, 5b, 5c and 5d.

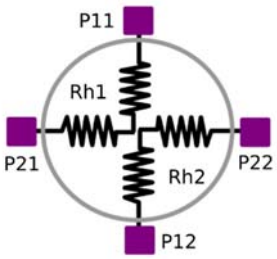

Fig. 5a. Double meander resistors diagram.

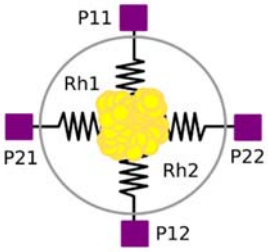

Fig. 5b. Idem Fig. 5a with the sensitive film (yellow).

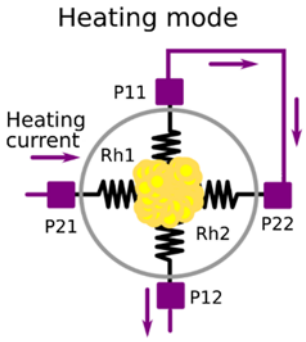

Fig. 5c. Diagram of the double meander resistors in heating mode: Rh1 and Rh2 resistors are connected in series.

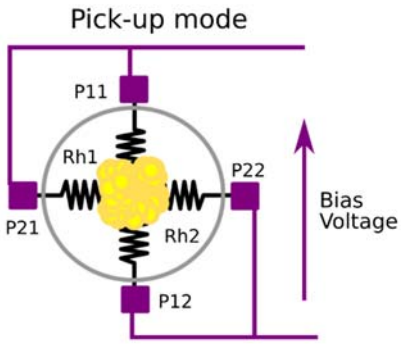

Fig. 5d. Diagram of the double meander resistors in pick-up mode: the electrodes of each resistor (Rh1 and Rh2) are short circuited.

The acquired data are presented, stored and used to calculate the analyte concentration periodically repeating this process according to the required application. A time plot corresponding to the described signals is shown in Fig. 6. It is qualitatively observed the difference between the heating times (heating mode) and the measurement of the sensitive film (pick-up mode). The electrodes, configured as heaters, excite the sensitive film only a few milliseconds. The sensitive film can reach a temperature of about 350 ºC to heat and clean the system to avoid gases that could interfere the measurements. Before measuring the sensitive film resistivity, a preheating is performed at ~250 ºC to allow evaporation of interfering molecules.

Once removed the heating power (heating mode), the film resistivity is measured with the signal conditioning circuit in pick-up mode, for a short time (less than one millisecond) after the heating effect is completed. Fig. 7 shows the described timing.

Fig. 6. Double meander resistors diagram.

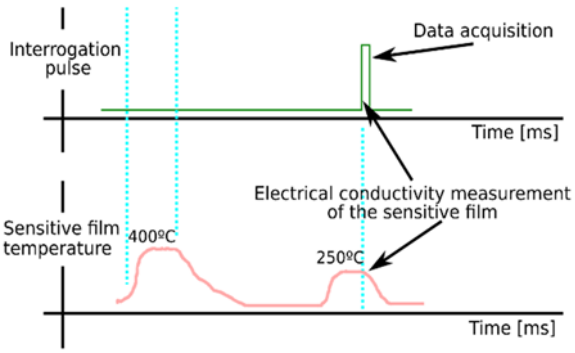

Fig. 7. Double meander resistors diagram.

Fig. 8 is an infrared micrograph showing the different temperature stages of the heater from room temperature to working temperature.

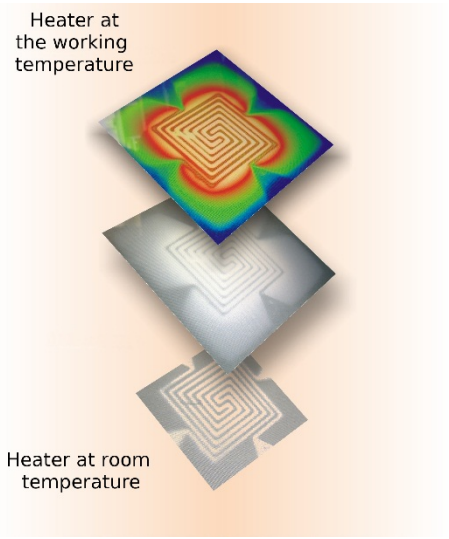

Fig. 8. Infrared images showing the heater different temperature stages a) heater image at Tw and b) heater image at room temperature.

The film temperature does not change fast due to the inertial effect of the system. After the heating time, a temperature value close to the preheating is maintained [20]. During this short time, the sensitive film can be biased to measure its resistivity, which is proportional to the adsorbed gas concentration.

3. Conclusions

The nanocrystalline pure, Al-doped or In-doped SnO_2 was synthesized with different crystallite size (Ø: crystallite diameter) to build resistive type gas sensors to detect: H_2, CO and VOCs. Synthesis was performed by gel-combustion method [Ø = 9 nm-15 nm] and by reactive oxidation with H_2O_2 [Ø = 2 nm - 9 nm]. Several techniques: DRX, BET isotherms adsorption method and HRTEM were used to characterise the microstructural and morphologic properties of the pure and doped nanocrystalline SnO_2. The calcination temperature produced an increase of grain size contributing to decrease the specific absorption area. The analysis of DRX spectra of doped SnO_2 with different crystallite size, always enabled to identify the structure of the crystallographic phase of tetragonal rutile as found in pure SnO_2. HRTEM micrographs show nanoparticles (with very small Ø), with rounded borders and high defects density, which are homogeneously distributed. Calcination at higher temperature caused larger size crystallites exhibiting a faceted form and with considerably minor defects density. Sensors to detect H_2, built with pure nano-SnO_2, showed a ~35 % higher sensitivity in

comparison with that of reference sensors. The working temperature (Tw) decreased to ~180 ºC - 200 ºC according to the smallest crystallite size. An electronic switching system was developed and applied to sensors, alternatively measuring the sensor resistivity proportional to the adsorbed gas concentration and setting the working temperature. Details of the MEMS microheater were carefully described.

Acknowledgements

Thanks are given to Eng. Federico Checozzi (UTN-FRH) for his help in the characterisation of micro-heaters and to Techn. Daniel E. Gasulla for his valuable work to build the protopypes and special devices. The authors thank to Damian Fernández for his thermography assistance at the Images Control Laboratory (CITEDEF).

References

[1]. L. B. Fraigi, D. G. Lamas, N. E. Walsöe de Reca, Quím. Analít. (España), 18, Suppl. 1, 1999, pp. 71-75.

[2]. L. B. Fraigi, D. G. Lamas, N. E. Walsöe de Reca, Solid State Microsensors for Environmental Monitoring, *CYTED*, Proy. IX.2, Ed. Control S. R. L., Bs. As., 1999, pp. 57-72.

[3]. L. B. Fraigi, PhD Thesis (Engin.) *FI-UBA*, 2006.

[4]. N. E. Walsöe de Reca, Anales Academia Nacional de Ciencias Exactas, Físicas y Naturales, *ANCEFyN*, 59, 2007, pp. 59-93.

[5]. L. B. Fraigi, D. G. Lamas, N. E. Walsöe de Reca, Novel method to prepare nanocrystalline SnO2 powders by a gel-combustion process, *Nanostruct. Mater.*, 11, 1999, p. 311-318.

[6]. L. B. Fraigi, D. G. Lamas, N. E. Walsöe de Reca, Comparison between two combustion routes for the synthesis of nanocrystalline SnO2 powders, *Mater. Lett.*, 47, 2001, p. 262-262.

[7]. M. F. Bianchetti, I. Bracko, S. D. Skapin, N. E. Walsöe de Reca, Nanocrystalline Tin Oxide to be Applied in a Gas Sensor, *Sensors & Transd. J.* 137, 2, 2012, pp. 155-164.

[8]. M. Cabezas, D. G. Lamas, E. Cabanillas, N. E. Walsöe de Reca, Method to build a Gas Sensor with nanostructured Al2O3-doped SnO2 to sense CO (gas), *R. A. Patent P20130101356*, Dec. 2013, in procedure.

[9]. M. Bianchetti, N. E. Walsöe de Reca, Gas sensor built with pure nanocrystalline SnO2 to sense H2, *Patente R. A. P 20130100781*, in procedure.

[10]. M. Bianchetti, M. E. Fernández, R. Juárez, N. E. Walsöe de Reca, Gas sensor de gas built with nanocrystalline In2O3-doped SnO2 to sense VOCs, *Patent R. A. P2013101426*, in procedure.

[11]. N. Yamazoe, J. Fuchigami, M. Kishikawa, T. Seiyama, Interactions of tin oxide surface with O2, H2O AND H2, *Surf. Sci.*, 86, 1979, pp. 335-344.

[12]. Yu. A. Dobrovolskii, G. V. Kalinnikov, Oxygen chemisorption by SnO2-based oxide electrodes in solid electrolytes, *Élektrokhimiya*, 28, 10, 1992, pp. 1567-1575.

[13]. Y. Shimidzu, M. Egashira, Basic concepts and challenges of semiconductor gas sensors, *MRS Bulletin*, 26, 4, 1999, p. 18-24.

[14]. N. E. Walsöe de Reca, M. F. Bianchetti, C. L. Arrieta, *Sensors and Actuators, B (Chemical)*, 2014, Vol. 190.

[15]. G. E. Lascalea, Materials Science and Technology, PhD Thesis, *Inst. Jorge Sabato, CNEA-UNSAM*, 2008.

[16]. M. F. Bianchetti, N. E. Walsöe de Reca., Novel method to synthesize nanostructured metallic oxides, *R. A. Patent P20130100781*, in procedure.

[17]. L. T. Alaniz, C. L. Arrieta, M. F. Bianchetti, C. A. Gillari, J. F. Giménez, H. A. Lacomi, D. F. Valerio and N. E. Walsöe de Reca, Gas sensor provided with a heating device and the method to sense, *R. A. Patent P-070105987*, granted on December 28th, 2013.

[18]. G. Cardinali, L. Dori, M. Fiorini, I. Sayago, G. Faglia, C. Perego, G. Sverbeglieri, V. Liberati, F. Maloberti, D. Tonietto, Annual Report, *Consiglio delle Recherche, LAMEL*, 1998, pp. 71-74.

[19]. J. F. Giménez J. F, C. A. Gillari, C. A Valerio, D. F. Gasulla, L. T. Alaniz, H. A. Lacomi, C. L. Arrieta., Pampa III Electronic Nose, *The Journal of the Argentine Chemical Society*, Vol. 93, 1/3, 2005, pp. 115-122.

[20]. D. Briand, A Krauss, B van der Schoot, U. Weimar, N. Barsan, W Göpel, N. F. Rooij, Design and fabrication of high-temperature micro-hotplates for drop-coated gas sensors, *Sensors &Actuators B.*, 68, 2000, pp. 223-233.